DØnote 4595-CONF

Search for R-parity violated supersymmetry in the 2 electrons + taus final state (λ_{133} coupling)

The DØ Collaboration
URL http://www-d0.fnal.gov
(Dated: November 12, 2004)

Data collected from September 2002 to mid of March 2004 by the DØ experiment in Run II at Fermilab Tevatron $p\bar{p}$ collider have been used to search for two electrons plus taus final states accompanied by missing transverse energy. These topologies are expected to arise if R-parity is violated and the lightest neutralino is allowed to decay through λ_{133} coupling. Data corresponding to an integrated luminosity of $198.7 \pm 12.9\, pb^{-1}$ at a center of mass energy of 1.96 TeV have been analyzed. Preliminary limits as a function of $m_{\tilde{\chi}_1^0}$ and $m_{\tilde{\chi}_1^\pm}$ are set, since the expected number of events is in agreement with the standard model expectations.

I. INTRODUCTION

Although the standard model has obtained remarkable success, there are strong arguments to consider it as a low energy effective theory. The most popular extension of the standard model is supersymmetry. Supersymmetry postulates the existence of a symmetry between fermions and bosons, thus doubling the number of known particles. It provides the necessary cancellation of quadratic divergences which appear in loop corrections to the masses especially in the case of the Higgs boson. Supersymmetry by itself does not impose the conservation of leptonic and baryonic numbers. The R-parity number defined as $(-1)^{3B+L+2S}$ was introduced to solve this problem. However the gauge symmetry of the MSSM (minimal supersymmetric standard model) allows to write terms in the superpotential which violate R-parity. One can write the R-parity violating part of the lagrangian as follows:

$$\lambda_{ijk}(L_iL_j)E_k^c + \lambda'_{ijk}(L_iQ_j)D_k^c + \lambda''_{ijk}(U_i^cD_j^cD_k^c) \tag{1}$$

These terms do violate the baryon number B (by the 9 λ''_{ijk} couplings) and the lepton number L (by the 9 λ_{ijk} couplings and the 27 λ'_{ijk} couplings).

In this note we have considered the case where the R-parity violating term violates only the leptonic number with a λ_{133} coupling $\neq 0$. The framework of this work is the so-called weak limit of R-parity violation, where the R-parity violating couplings are considerably smaller than the gauge couplings [1]. Most production and decay processes will thus take place with R-parity conserving couplings, only the LSP is allowed to decay into Standard Model particles. In the case of a λ_{133} coupling $\neq 0$, the lightest supersymmetric particle, the neutralino, decays into one tau, an electron or a tau and a neutrino (as shown on Fig. 1). Therefore the corresponding final state contains four charged leptons accompanied by missing transverse energy. In this note we look for final states with two electrons and at least one tau identified in its hadronic decay modes (narrow jet with low multiplicity). Section II describes the dataset and MC samples, section III the estimate of the tau identification efficiency, section IV the final state selection and section V the results.

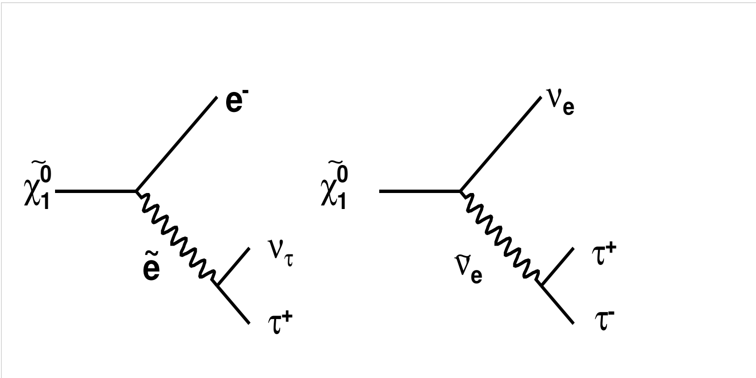

FIG. 1: $\tilde{\chi}_1^0$ *RpV decays with* λ_{133} *coupling.*

II. DATASET AND MC SAMPLES

The data used were collected with the Run II DØ detector, from September 2002 to mid of March 2004 and correspond to an integrated luminosity of $198.7 \pm 12.9\,pb^{-1}$. The analysis sample consists of events triggered by single or dielectron triggers, based on the presence of calorimeter clusters associated or not to a track.

Signal events have been produced with SUSYGEN generator [2] which uses SUSPECT [3] for the evolution of the Renormalization Group Equations. Events have been generated for different points in the mSUGRA parameter space ($sign(\mu) = +1$, $A_0 = 0$, $tan\beta = 10$, $m_0 = 80$). For the signal simulation, a reference value of $\lambda_{133} = 0.003$ has been used, which corresponds to the present experimental limit [6]. With this λ_{133} value the LSP decays within few mm's of the primary vertex. To optimize the selection of the two electrons plus taus final states, parameter combinations where the stau is lighter than the $\tilde{\chi}_1^\pm$ have been considered. For this mass hierarchy, additional taus from the cascade are expected to enhance the tau multiplicity of the final state. Physical properties of the signal points can be found in table I.

The main background sources are $Z/\gamma^* \to ee$, $Z/\gamma^* \to \tau\tau$, $W \to e\nu$, $W \to \tau\nu$ where QCD jets are misidentified as taus or electrons or mismeasured as missing transverse energy. These Monte-Carlo samples have been generated with PYTHIA 6.202 and the particle data function CTEQ5L.

TABLE I: *Masses (Gev/c^2) and cross sections (pb) for fully simulated events generated with SUSYGEN in the mSUGRA framework. N stands for neutralino and C for Chargino. A K-factor of 1.2 is applied to obtain NLO gaugino's cross sections as described in [4].*

m_0	$m_{1/2}$	$sign(\mu)$	$\tan(\beta)$	$m_{\tilde{\chi}_1^0}$	$m_{\tilde{\chi}_1^\pm}$	$m_{\tilde{\tau}}$	σ_{NN}	σ_{CC}	σ_{NC}	σ_{tot}	σ_{tot} (NLO) (pb)
80	160	1	10	58.	101.6	101.2	0.027	0.55	0.91	1.5	1.8
80	170	1	10	62.5	110.45	103.3	0.02	0.39	0.63	1.04	1.25
80	180	1	10	67.	119.2	105.5	0.014	0.28	0.44	0.75	0.9
80	190	1	10	71.5	128	107.8	0.01	0.2	0.32	0.53	0.64

III. TAU IDENTIFICATION IN HADRONIC MODES

This section describes the method used to identify taus in their hadronic decay modes and the study done to estimate the efficiency of the identification technique. For this purpose a specific data sample has been used made of events with isolated muons. The correction factor obtained in this section to take into account the differences between Monte-Carlo and data is used in the search for R-parity violated supersymmetry with λ_{133} coupling.

A. Introduction

Hadronic decay modes of taus can be seen as narrow jets (with essentially one or three tracks) with specific electromagnetic energy fraction to hadronic energy fraction ratios. Based on these characteristics we consider several variables : transverse and longitudinal shower shape, isolation criteria, electromagnetic ratio, sub-clusters at the maximum of the shower width. A set of neural networks has been developed, using these discrimating properties, in order to separate taus in their hadronic modes from QCD jets. Two neural networks have been designed, in order to recognize single track taus according to the decay signature they leave in the detector[7].

- type 1 : single track with calorimeter cluster but no electromagnetic sub-clusters ($\tau \to \pi\nu$ like).
- type 2 : single track with calorimeter cluster and electromagnetic sub-clusters ($\tau \to \pi(n\pi^0)\nu$ like, n>= 1).

In addition to this set of neural networks a further neural network was developed in order to take care of the electron contamination which can fake taus essentially of the second type. We refer as NN^{QCD} the neural network trained on QCD background, while NN^e denotes the neural networks designed to remove the electron background. The NN^{QCD} have been trained on Monte-Carlo generated single taus for the signal and jets recoiling against non-isolated muons from data for background. The NN^e has been trained on the same signal sample and on $Z \to ee$ Monte-Carlo for the background sample.

Muons faking taus in the calorimeter are removed by taking into account the shower shape of the energy deposition in the hadronic cluster. The so called $\mathcal{R}_\mu$ variable is used, $\mathcal{R}_\mu = (E^\tau - E^{trk}_{CH})/p^{trk}_T > 0.7$ where E^τ is the visible energy deposited by the tau in the calorimeter, E^{trk}_{CH} the hadronic energy in a 5x5 window around the track in the outer part of the calorimeter and p^{trk}_T the total transverse energy of the tau track.

B. Efficiencies of neural networks in data

We have used a data sample to estimate the neural networks efficiency ratio of data to Monte-Carlo for taus of type 1 and 2. An enriched sample of taus, essentially originating from the process $Z \to \tau\tau \to \tau_{hadr}\mu$ is selected. A detailed study of this physics process can be found in [5]. μ-τ pairs are chosen if they are back to back with a difference in azimuthal angle $\Delta\phi_{\mu\tau} > 2.7$ and if their invariant mass [8] lies between 40 and 80 GeV/c^2, since transverse energy is carried away by the neutrinos. Loose cuts on the lepton momenta are as well applied : $p_{T_\tau} > 7$

GeV/c, $p_{T_\mu} > 14$ GeV/c.
The events are required to contain only one medium quality muon ($n_\mu = 1$) in order to minimize the $Z \to \mu\mu$ contribution. Muons faking taus have also been removed by using the $\mathcal{R}_\mu$ variable. The cut on the neural network for electrons is applied on the tau candidate, and events with a tau candidate in the inter-cryostat region were discarded, in order to reduce the $Z \to \tau\tau \to \mu e$ contribution.

This sample is separated in two subsamples:
1) same sign sample referring to events in which the sign of the muon and of the charged hadron (single track type) are the same. This sample is poor in hadronic tau decay modes.
2) opposite sign sample which includes $Z \to \tau\tau \to \tau_{hadr}\mu$ as well as QCD type jets.

Using these 2 samples, as well as a Monte Carlo sample of $Z \to \tau\tau \to \tau_{hadr}\mu$ and a Monte Carlo sample of $Z \to \mu\mu$, we have fitted the tau candidate transverse momentum (defined as the transverse visible energy deposit in the calorimeter) distribution in order to estimate the contribution of $Z \to \tau\tau \to \tau_{hadr}\mu$ in our opposite sign sample. A minimization of a chisquare function has been used to perform this fit, leading to a relative error of 10% on the $Z \to \tau\tau \to \tau_{hadr}\mu$ content. The $Z \to \mu\mu$ contribution is estimated independently as described in section III C and kept constant in the fit. Fig. 2 shows the p_T spectrum with the evaluated fraction of QCD jets, $Z \to \mu\mu$ and $Z \to \tau\tau \to \tau_{hadr}\mu$ events.

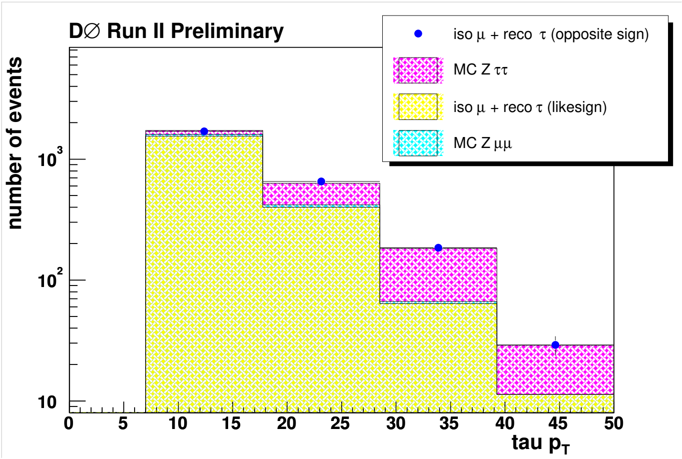

FIG. 2: *Transverse momentum distribution of the tau candidates.*

Figures 3-4 are examples of good understanding of discriminating variables before applying the cut on the outputs of the neural networks trained on QCD background. Figures 5-7 show the discrimating variables and final agreement of the tau candidate transverse momentum distribution after the neural network cuts. The $Z \to \tau_{hadr}\mu$ and QCD contributions are scaled to the ratio obtained by the fit on the p_T spectrum. The correction factor used to describe the difference in efficiency of the NN^{QCD}'s in MC and data, derived in section III C is applied in addition on the last Figures 5 to 7.

Figures 3 and 5 show the transverse energy weighted cluster width, defined by $\sqrt{\Sigma_i^n(\frac{\Delta\phi^2 E_{T_i}}{E_T} + \frac{\Delta\eta^2 E_{T_i}}{E_T})}$. This cluster width is the transverse energy weighted root mean square of the distance of the n cluster towers in the $\eta - \phi$ space with respect to the main cluster direction. E_{T_i} represents the transverse energy of each tower in the cluster and E_T the total transverse energy of the calorimeter cluster. Figures 4 and 6 show the cluster isolation, defined by the transverse energy difference between two cones of radius $\mathcal{R} = \sqrt{\eta^2 + \phi^2} = 0.5$ and 0.3, divided by the transverse energy of the inner cone. The tau contribution can be seen as expected among candidates with a small cluster width and an isolated calorimeter cluster.

C. Muon contamination

In order to estimate the number of $Z \to \mu\mu$ events, where one muon is misidentified as a tau in our opposite sign sample of $Z \to \tau_{hadr}\mu$ events, the invariant mass of the tau track plus muon is considered. The number of events in

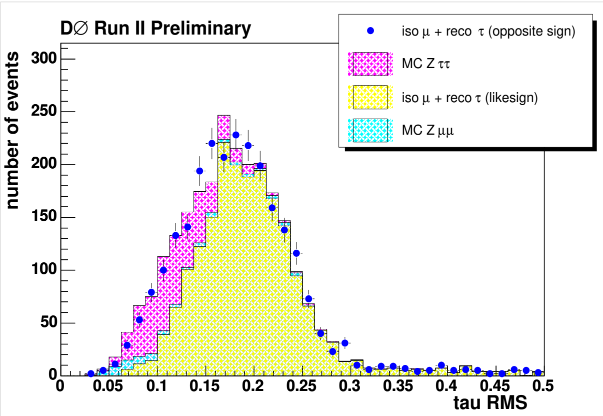

FIG. 3: *Transverse energy weighted cluster width (as defined in the text).*

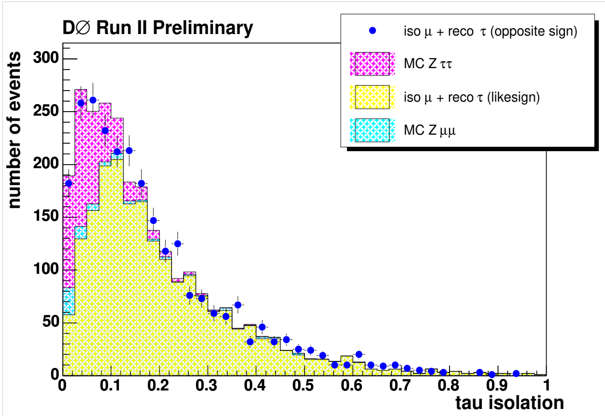

FIG. 4: *Cluster isolation (as defined in the text).*

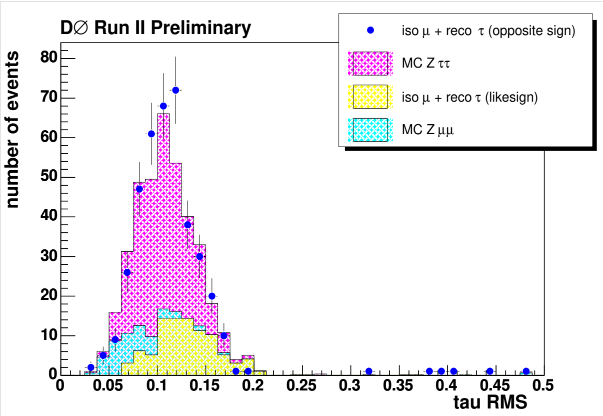

FIG. 5: *Transverse energy weighted cluster width after cuts on neural networks.*

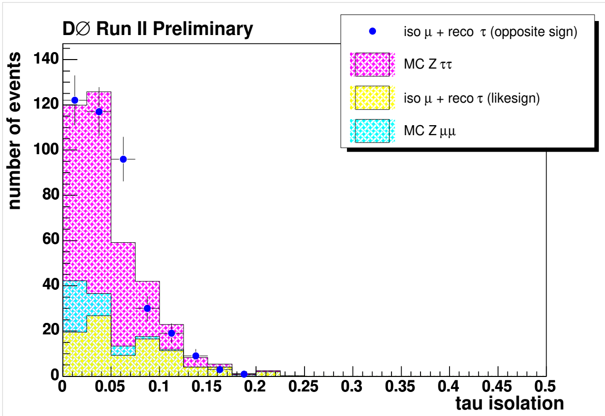

FIG. 6: *Cluster isolation after cuts on neural networks.*

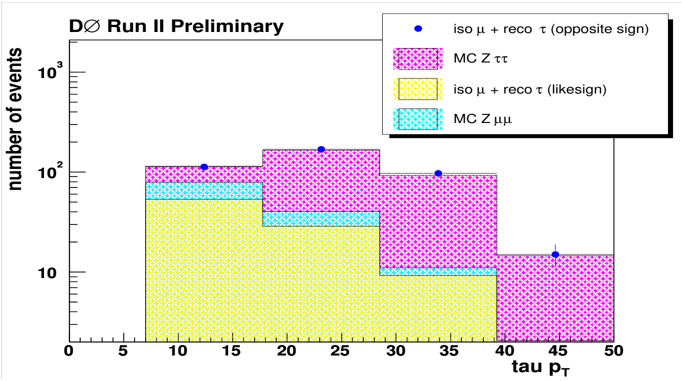

FIG. 7: *p_T distribution of the tau candidates after cuts on neural networks.*

the Z peak mass window (i.e $M_{\mu\tau_{trk}} \in$ [81,101] GeV/c^2) is compared to a $Z \rightarrow \mu\mu$ MC sample while all preselection cuts to enhance the $Z \rightarrow \tau_{hadr}\mu$ content in the opposite sign sample are applied. It is found that the opposite sign data sample contains 74 $\pm$ 14 $Z \rightarrow \mu\mu$ events among the 2568 selected opposite sign $\mu - \tau$ pairs.

From Table II the following correction factor to take into account for the differences between MC and data is calculated, using the number obtained after the cuts on neural networks:

$$f_\tau = \frac{N_{Z\to\tau\tau}(data)}{N_{Z\to\tau\tau}(MC)} = \frac{(N^{OS}_{\mu\tau}(data) - N^{SS}_{\mu\tau}(data) - N_{Z\to\mu\mu})}{N_{Z\to\tau\tau}(MC)} = \frac{264}{329} = 0.8$$

This factor has been folded into Monte-Carlo and applied in Figures 5 to 7. The error on this correction factor is mainly due to the error of 10% on the estimate of the $Z \to \tau\tau$ content before applying the neural networks.

TABLE II: *Estimate of $Z \to \tau\tau$ content before and after applying the cuts on the neural networks.*

	preselection + $\mathcal{R}_\mu > 0.7$ + $n_\mu = 1$	+ $NN^{QCD} > 0.9$
$N^{OS}_{\mu\tau}(data)$: number of $\tau - \mu$ pair of opposite sign	2568	396
$N^{SS}_{\mu\tau}(data)$: number of fitted $\tau - \mu$ pair of same sign	2025	93 ± 2
$N_{Z\to\tau\tau}(MC)$: number of fitted $Z \to \tau\tau$	468 ± 43	329 ± 30
$N_{Z\to\mu\mu}$: number of estimated $Z \to \mu\mu$	74 ± 14	39 ± 8

IV. SELECTION OF THE E+E+TAUS FINAL STATE

A. Cut flow

The event selection proceeds in four steps. The first step requires two electrons with an invariant mass higher than 18 GeV/c^2. The electron identification relies on the electromagnetic energy fraction, isolation and shower shape of the calorimeter cluster. A likelihood estimator using the track match information is further used to reduce the contamination from jets and to distinguish between electrons and photons. At this first stage the invariant mass is checked to be in agreement with the SM processes and QCD multi-jets processes where jets are misidentified as electrons. The QCD estimate is described in the next section. The invariant mass is then required to be less than 80 GeV/c^2 in order to supress $Z \to ee$ events. The third selection reduces the dataset to events containing in addition at least on hadronic tau. The signal we look for exhibits moderate missing transverse energy. QCD events may also have moderate missing transverse energy due to jet energy mismeasurement. A useful variable is the ratio $ME_T/\sqrt{SE_T}$ which takes into account statistical flucuation of QCD jets energy mismeasurement (where ME_T is defined as the transverse missing energy and SE_T as the total scalar transverse energy). To select events with significant missing transverse ernergy a cut $ME_T/\sqrt{SE_T} > 1.5$ is then applied. The distributions of $ME_T/\sqrt{SE_T}$ and invariant dielectron mass are shown in Fig. 8 to 9 at the preselection cut of two electrons. The dark triangles represent the data. The detailed cut flow of the analysis is summarized in table III.

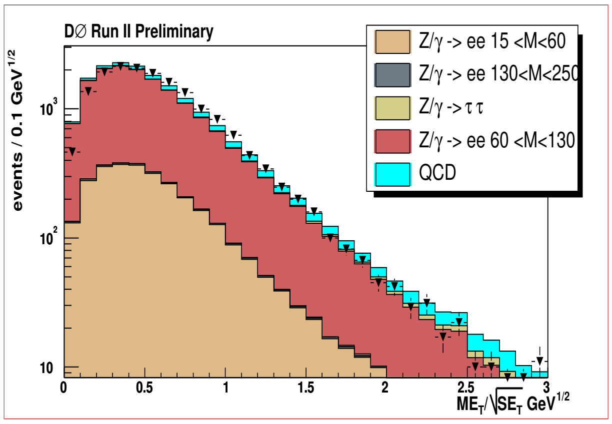

FIG. 8: $ME_T/\sqrt{SE_T}$.

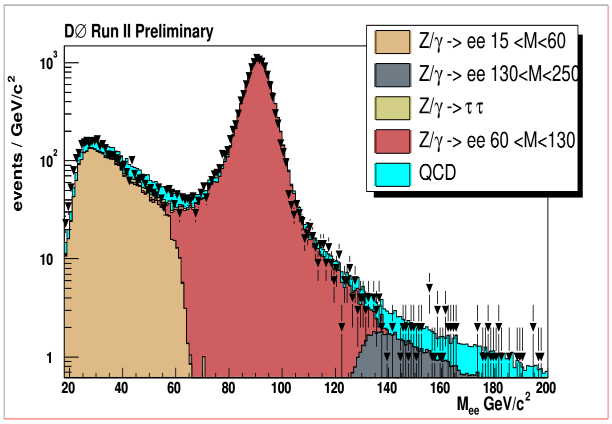

FIG. 9: *Dielectron invariant mass.*

TABLE III: *Cut flow of the analysis.*

(III.1) 2 electrons preselection	$p_{T_1} > 10$, $p_{T_2} > 10$ GeV/c electrons are required to come from the primary vertex $\lvert z_{vtx}(elec) - z_{vtx}\rvert < 1$cm M_{ee} >18 GeV/c^2
(III.2)	M_{ee} <80 GeV/c^2
(III.3) at least one hadronic tau	$p_{T_\tau} > 7 GeV/c$ type 1 or type 2 should be outside the inter-cryostat region anti QCD jet : NN^{QCD}_{type1} or $NN^{QCD}_{type2} > 0.9$ anti electron background : $\Delta\phi_{e\tau} < 0.1$, NN^e >0.9 anti muon background : $\Delta\phi_{\mu\tau} < 0.1$, $\mathcal{R}_\mu > 0.7$
(III.4) Anti-Drell Yan and QCD cut	$ME_T/\sqrt{(SE_T)} > 1.5$

B. QCD background

The number of QCD events, where two jets are misidentified as two electrons is estimated by considering the number of like sign electrons in our selection sample at the cut level III.1 (see table III). Such a sample contains little $Z \to ee$ events and is dominated by QCD events. We assume that $N^{OS}_{QCD} = N^{SS}_{QCD} = N^{SS}_{data} - N^{SS}_{MC}$ where N^{SS}_{MC} refers to the number of same sign events found in all standard model Monte-Carlo except QCD. N^{SS}_{MC} has been found to be almost negligible. In order to get an estimate of the number of QCD events at each level of the analysis, a QCD sample is defined. The like sign dielectron sample is not directly used since the signal can also contain two equal sign electrons, if one electron stems from a tau for instance. This sample consists of events containing two fake electrons, defined by inverting the cuts used to identify electrons. This sample of fake electrons has then been normalized to the number of estimated QCD with the like sign method ($N_{QCD} = 2 * (N^{SS}_{data} - N^{SS}_{MC})$). Fake electrons have been removed of the QCD sample if they match a tau candidate in a $\Delta\mathcal{R} = \sqrt{\Delta\eta^2 + \Delta\phi^2} > 0.3$ cone in order not to count twice the same electromagnetic cluster.

V. RESULTS AND CONCLUSION

A. Comparison between data and expectations from Monte-Carlo

Figures 10 to 11 show the $ME_T/\sqrt{(SE_T)}$ distribution, and tau type distribution at cut III.3. The number of data and expected events from SM processes are given in Table IV. The tau data/MC efficiency factor computed in section III C is applied in MC for events where taus are selected. The number of expected events in standard model MC with two electrons and two taus is equal to zero, as well as the number of observed events in data. The quoted errors include systematic errors combined with the statistical errors.

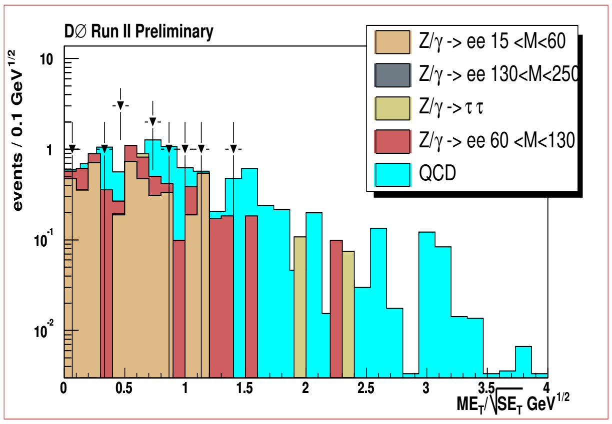

FIG. 10: $ME_T/\sqrt{(SE_T)}$ *at the two electrons plus tau cut.*

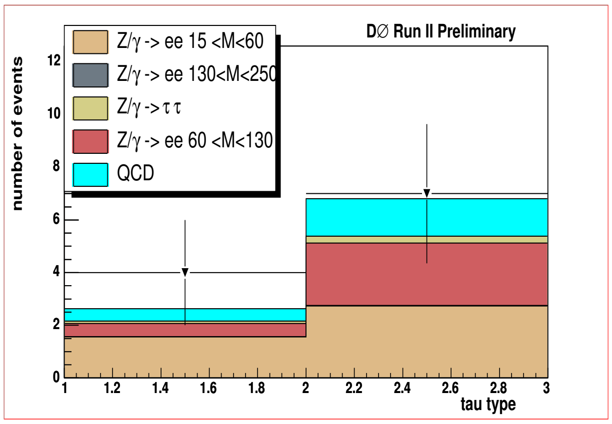

FIG. 11: *Selected tau type.*

The systematic errors taken into account in Table IV stem mainly from the error of 12.5 % on the tau Data/MC efficiency correction factor, followed by the 6.5% error on the luminosity. Following effects have also been considered:

- the uncertainties due to the correction factor between data and MC for electrons, about 2%.
- the uncertainties on the trigger efficiency for the different Monte-Carlo samples (5% for the $Z \to ee$ process with $M_{ee} \in$ 15-60 GeV/c^2)
- the errors on the cross-sections used for the SM background processes (between 5% and 8% error).

TABLE IV: *Number of data events observed and background events expected for the different cuts used in the selection. The systematic errors include errors on efficiency, luminosity and cross sections.*

SM process	2 e $M_{ee} > 18$	+ $M_{ee} < 80$	+ $\tau >= 1$	+ $ME_T/\sqrt{(SE_T)}$ >1.5
$t\bar{t}$	5.63 ± 0.42	3.07 ± 0.24	0.01± 0.01	0.01± 0.01
W-> $e\nu$ + j	4.78 ± 2.74	4.78± 2.74	0	0
W-> $e\nu$ + 2j	7.74 ± 1.73	6.73± 1.59	0	0
W-> $\tau\nu$ + j	0.46 ± 0.99	0.46± 0.99	0	0
W-> $\tau\nu$ + 2j	1.39 ± 1.6	1.39± 1.6	0	0
Z-> $\tau\tau$ 15-60	2.43 ± 0.81	2.38± 0.8	0	0
Z-> $\tau\tau$ 60-130	125.12 ± 11.45	123.86± 11.35	0.31± 0.21	0.25± 0.19
Z-> ee 15-60	2706.36 ± 348.74	2692.83± 347.08	3.82± 1.1	0
Z-> ee 60-130	13183.3 ± 1037.41	1050.16± 83.61	2.8± 0.69	0.27± 0.19
Z-> ee 130-250	81.84 ± 5.58	0.25± 0.03	0.01± 0	0
QCD	918 ± 30	699 ± 26.4	2.1 ± 1.15	0.5 ± 0.7
total of bkg	17037 ± 1094	4586.59 ± 356.13	9.08 ± 0.98	1.04 ± 1.42
DATA	17172	4907	11	0

B. Signal efficiency and limits

TABLE V: *Efficiencies for different SUSY points with systematic errors at different stage of the analysis. The systematic errors do not include the error on the cross sections.*

Acceptance %	2 e $M_{ee} \in$ (18,80)	+ τ >=1	+ $ME_T/\sqrt{(SE_T)}$ >1.5
$m_0 = 80$ $m_{1/2} = 160$ $m_{\tilde{\chi}_1^\pm} = 101.41$	9.22± 0.25	1.6± 0.24	1.24± 0.19
$m_0 = 80$ $m_{1/2} = 170$ $m_{\tilde{\chi}_1^\pm} = 110.45$	9.77± 0.23	2.14± 0.34	1.72± 0.27
$m_0 = 80$ $m_{1/2} = 180$ $m_{\tilde{\chi}_1^\pm} = 119.1$	9.87± 0.23	2.3± 0.36	1.67± 0.26
$m_0 = 80$ $m_{1/2} = 190$ $m_{\tilde{\chi}_1^\pm} = 128$	11.27± 0.25	2.85± 0.45	1.88± 0.3

TABLE VI: *Tests of exclusion on SUSY points for the two electrons plus at least one hadronic tau channel.*

	acceptance %	expected evts	$\sigma_{NN+CC+NC}$ (NLO) (pb)	σ_{95} (pb)
$m_0 = 80$ $m_{1/2} = 160$ $m_{\tilde{\chi}_1^\pm} = 101.41$	1.24± 0.19	3.69± 0.82	1.8	1.3
$m_0 = 80$ $m_{1/2} = 170$ $m_{\tilde{\chi}_1^\pm} = 110.45$	1.72± 0.27	3.55± 0.74	1.25	0.95
$m_0 = 80$ $m_{1/2} = 180$ $m_{\tilde{\chi}_1^\pm} = 119.1$	1.67± 0.26	2.45± 0.53	0.9	0.97
$m_0 = 80$ $m_{1/2} = 190$ $m_{\tilde{\chi}_1^\pm} = 128$	1.88± 0.3	2.02± 0.41	0.65	0.87

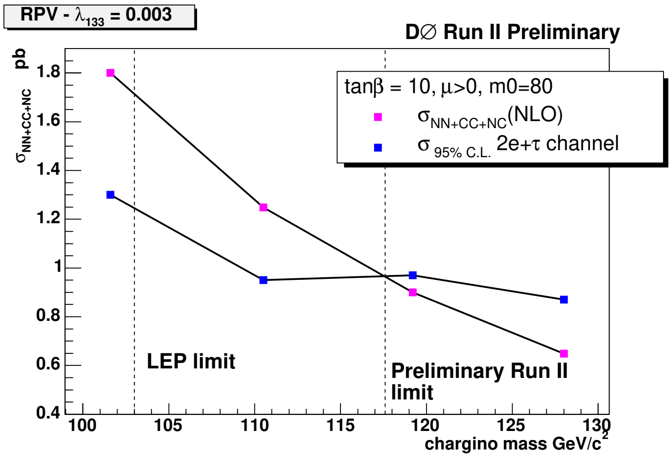

FIG. 12: *The 95% C.L. upper limit on the gaugino's production cross section ($\sigma_{95\%\,C.L.}$) is compared to the theoretical cross section ($\sigma_{NN+CC+NC}$) for fixed $tan\beta$ = 10, m_0 = 80 GeV/c^2 and positive μ as a function of the chargino mass.*

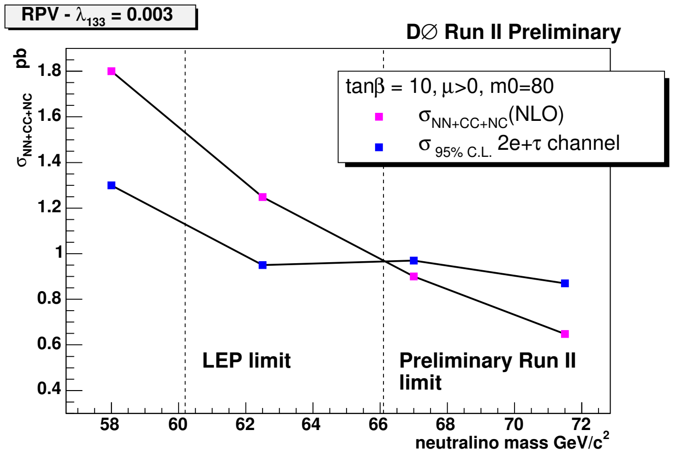

FIG. 13: *The 95% C.L. upper limit on the gaugino's production cross section ($\sigma_{95\%\,C.L.}$) is compared to the theoretical cross section ($\sigma_{NN+CC+NC}$) for fixed $tan\beta$ = 10, m_0 = 80 GeV/c^2 and positive μ as a function of the neutralino mass.*

The data seen is consistent with SM and instrumental backgrounds which suggests no evidence for $\tilde{\chi}_1^0$ pair production followed by decay with λ_{133} coupling. After all selections 0 events from data are seen while 1.04 $\pm$ 1.42 events are expected from SM physics processes and instrumental backgrounds. Using the results given in Tables IV and V and a bayesian technique, upper limits on the cross section with 95 % confidence limit are set. The results are summarized in table VI. In figures 12 and 13 we show the calculated limit as function of $m(\tilde{\chi}_1^{\pm})$ and $m(\tilde{\chi}_1^0)$. The reference values for the LEP limits of the chargino and neutralino masses have been taken out of [6]. This preliminary result allows to exclude at 95% C.L. the regions with $m(\tilde{\chi}_1^{\pm})$ <118 GeV/c^2, $m(\tilde{\chi}_1^0)$ < 66 GeV/c^2 for $\mu > 0$, $tan\beta = 10$, $m_0 = 80$, $m_{1/2} \in$ [160-190].

Acknowledgments

We thank the staffs at Fermilab and collaborating institutions, and acknowledge support from the Department of Energy and National Science Foundation (USA), Commissariat à l'Energie Atomique and CNRS/Institut National de Physique Nucléaire et de Physique des Particules (France), Ministry of Education and Science, Agency for Atomic Energy and RF President Grants Program (Russia), CAPES, CNPq, FAPERJ, FAPESP and FUNDUNESP (Brazil), Departments of Atomic Energy and Science and Technology (India), Colciencias (Colombia), CONACyT (Mexico), KRF (Korea), CONICET and UBACyT (Argentina), The Foundation for Fundamental Research on Matter (The Netherlands), PPARC (United Kingdom), Ministry of Education (Czech Republic), Natural Sciences and Engineering Research Council and WestGrid Project (Canada), BMBF (Germany), A.P. Sloan Foundation, Civilian Research and Development Foundation, Research Corporation, Texas Advanced Research Program, and the Alexander von Humboldt Foundation.

[1] V. Barger, M.S. Berger, P. Ohmann and R.J. Phillips, *Phys. Rev. D* 50, 4299 (1994); H. Baer, C. Kao and X. Tata, *Phys. Rev. D* 51, 2180 (1995).
[2] N.Godhane, S. Katsanevas, P. Morawitz, E. Perez *Susygen 3.00/43*
[3] A. Djaoui, J.-L. Kneur, G. Moultaka, hep-ph/0211331 (2002) *Suspect : a Fortran Code for the Supersymmetric and Higgs Particle Spectrum in the MSSM*
[4] W. Beenakker, M. Klasen, M. Krämer, T. Plehn, M. Spira and P.M. Zerwas, hep-ph/9903282 (1999) *The production of Charginos, Neutralinos, and Sleptons at Hadron Colliders*
[5] DØ collaboration, V. Abazov et al. *Measurement of* $\sigma * Br(Z/\gamma^* \rightarrow \tau\tau)$ *at* $\sqrt(s) = 1.96$ *TeV* in preparation for submission to PRL
[6] Th.D. Papadopoulou *talk at ICHEP 2002*

[7] type 3 taus have been discarded in this version of the analysis, since the QCD jet misidentification efficiency is high for this type of taus

[8] the calorimeter p_T of the tau is used to compute this invariant mass.